

# Supplementary Materials for

## Photon Momentum Transfer in Inhomogeneous Dielectric Mixtures and Induced Tractor Beams

Cheng-Wei Qiu, Weiqiang Ding, M. R.C. Mahdy, Dongliang Gao, Tianhang Zhang, Fook

Chiong Cheong, Aristide Dogariu, Zheng Wang, and Chwee Teck Lim

### **1. About the ray tracing method**

In order to calculate the light momentum transfer unambiguously, we calculate the optical force using a ray tracing method (RTM). This method has been used in one of our recent paper [Nat. Photon. **7** 787 (2013), the 2<sup>nd</sup> section in the supplementary material]. Here, we outline the main idea and procedure of this method again for the convenience of readers to follow. In the calculation, the incident light beam is regarded as a bundle of  $N$  optical rays ( $N$  was of the order of several thousands in our calculations), each ray carrying  $m$  photons with a momentum of  $m\mathbf{p}$  and energy of  $mE_0$ . Here  $\mathbf{p}$  and  $E_0 = \hbar\omega$  are the momentum and energy carried by a photon. Then, the momentum changes for each ray  $\Delta\mathbf{p}$  are calculated by a ray tracing method based on the Fresnel reflection and refraction formulations with the consideration of polarization, refractive indices, and incident angle. A ray experiences multiple reflections and refractions when it is incident onto the scatterer. During this process, the momentum change of the ray may be determined by accounting for the direction and strength of the transmissions and reflections:

$$\begin{aligned}\Delta\mathbf{P}_{\text{ray}} &= \Delta\mathbf{P}_{\text{ray},1} + \Delta\mathbf{P}_{\text{ray},2} + \dots \\ &= P_0 (R_1\mathbf{A}_{1r} + T_1T_2\mathbf{A}_{2t} + T_1R_2\mathbf{A}_{2r} - \mathbf{A}_{1i} + \dots)\end{aligned}$$

Here  $P_0$  is the amplitude of the momentum of the incident ray,  $\mathbf{A}_{ni,nt,nr}$  are the directional vectors along the incident, transmission, and reflection rays for the  $n$ -th refraction, the length of which is exactly equal to the refractive index value;  $T_{2,1}$  and  $R_{2,1}$  are energy transmission and reflection coefficients determined by the Fresnel formulas. For a given incident vector  $\mathbf{A}_i$ , the transmission and reflection vectors are determined by the following vector form of [1]

$$\begin{aligned}\mathbf{A}_t &= \mathbf{A}_i + Q \cdot \mathbf{n} \\ \mathbf{A}_r &= \mathbf{A}_i - 2n(n \cdot \mathbf{A}_i)\end{aligned}$$

Here  $\mathbf{n}$  is the outward normal unit vector,  $Q$  is a function of the incident angle  $\varphi$  and the refractive indices  $Q = \sqrt{n''^2 - n'^2 + n'^2 \cos^2 \varphi} - n' \cos \varphi$ ,  $n'$  and  $n''$  denote the refractive indices of incident and transmission sides, respectively. Then we can calculate the total changes of the momentum of the incident light beam as  $\Delta \mathbf{P} = \sum \Delta \mathbf{P}_{\text{ray}}$  where only the rays hitting the scatterer are involved. Then the optical force on the scatter can be derived straightforwardly by  $\mathbf{f} = -\Delta \mathbf{P} / \Delta t$ .

## ***2. Momentum formula to be used in current situation***

In the main text, the optical forces were calculated using the Minkowski momentum in ray tracing method. In the long standing debate of Minkowski and Abraham momentums, both of them have been supported by some experiments [2, 3]. However, it is more reasonable in the current paper to use the Minkowski formula in the force calculation due to the following reasons. First, our target is not only to prove the suitability of a certain momentum formula, but also to find the observable *momentum transferred to the object only* (excluding those transferred to the environment). In the existing experiments (e.g., Gibson's photon drag experiment [4], Jones and Richards's experiment [5], Jones and Leslie's experiment[6]), the Minkowski momentum can directly explain the experimental observations. Second, the current configuration is similar to a one-surface (semi-infinite) structure. When the light illuminates on an object, the light is transmitted into the object which then encounters an object-water interface (with low contrast in refractive indices). Since the refractive index ratio of the object with water is very small, the reflection and momentum changes are also small (less than 10% for either momentum formula). One may also imagine the extreme case of  $n_{\text{water}} = n_{\text{object}}$ , where the light will only encounter one interface between air and the object. For such a structure, the front interface (air-object surface) itself (excluding the back interface, i.e., object-water interface) will experience a backward force [7], which can be evaluated by the Minkowski formula.

In summary, although there is a long standing controversy for the momentum of a photon in medium (it is believed that this controversy has been resolved in Ref [8]), when the momentum is transferred to the front surface of an object (excluding those transferred to the back surface), Minkowski formula will show us results in agreement with the experimental observations. In other words, the momentum is not required to debate in order to investigate the tractor beam

behavior in the main text.

On the other hand, one may wonder what the magnitude of force is if it is calculated by other momentum formulas. Different momentum means different parameter  $\alpha$  in the following momentum formula

$$p = \alpha p_0 = \alpha \frac{\hbar\omega}{c} \quad (1)$$

where  $\hbar$ ,  $\omega$  and  $c$  are reduced Planck constant, angular frequency, and light velocity in vacuum, respectively.  $p_0 = \hbar\omega/c$  is the momentum of the photon in vacuum. The parameter of

$\alpha$  is  $n$ ,  $1/n$  and  $(4n + 7n^2 - n^4)/(10n)$  for Minkowski[9], Abraham[10], and Peierls formulas[11], respectively. FIG. 1s (a) shows that the Minkowski and Abraham momentums are the upper and lower boundaries, respectively; while the Peierls momentum is about the average value of them.

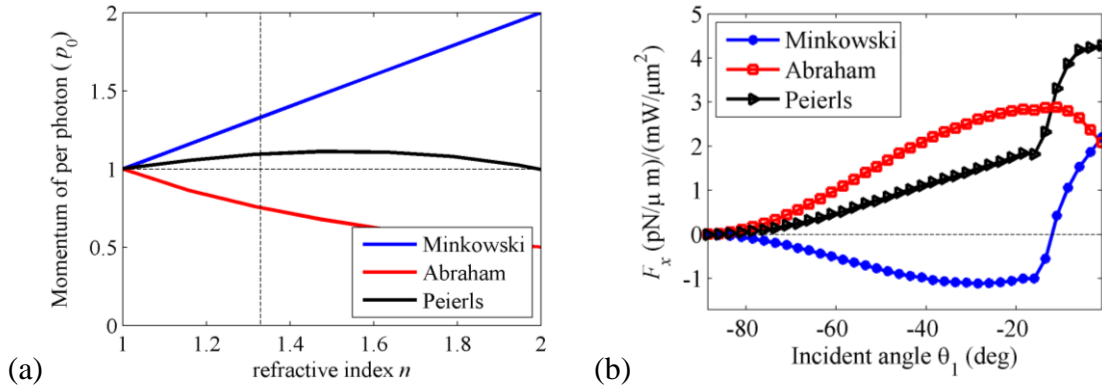


FIG. 1s (Color online). (a) Changes of momentum per photon in materials with a refractive index  $n$  for Minkowski (blue), Abraham (red) and Peierls (black) formulations, respectively. (b) Optical forces (s-polarization) calculated by ray tracing simulations when Minkowski (blue), Abraham (red), and Peierls (black) momentums are used.

Using the above momentum formulations, the forces of  $F_x$  can be calculated by using the ray tracing method, and the results are shown in FIG. 1s(b). It is seen that only the Minkowski momentum results in a negative pulling force in a wide range of incident angles while those of Abraham and Peierls momentums result in positive pushing forces regardless of the incident angles.

### 3. A short overview on some force formulas:

The mechanical momentum ( $P_{med}$ ) which is gained by a single photon (from the background medium), when it transfers momentum to an embedded particle, can be expressed as:

$$P_{med} = [(n_p - n_p^{-1}) \hbar \omega / c]$$

where  $n_p$  is the phase refractive index in non-dispersive medium [3] (in our main text  $n_p$  is for the background medium).  $P_{med}$  stands for the momentum and  $\hbar$  is the reduced Plank constant. According to [3],  $P_{med}$  originates from extra Abraham term,  $f^A$ ; this  $f^A$  can be expressed as:

$$\mathbf{f}^A = (n_p^2 - 1) \frac{\partial}{\partial t} \left( \frac{\mathbf{E} \times \mathbf{H}}{c^2} \right)$$

The total Abraham volume force density ( $f_A$ ) is written in this way:

$$\mathbf{f}_A = \mathbf{f}_H + \mathbf{f}^A$$

$$\text{where } \mathbf{f}_H = \left( -\frac{1}{2} E^2 \Delta \epsilon - \frac{1}{2} H^2 \Delta \mu \right).$$

In above Equation;  $f_H$  is the Helmholtz force term which is used in the linear momentum conservation Equation of Minkowski formulations [12].  $\Delta \epsilon$  and  $\Delta \mu$  in Helmholtz force density present spatial variation of permittivity and permeability respectively, especially in interfaces where permittivity and permeability present discontinuity. Hence Helmholtz force is a purely surface force density. On the other hand, it is well known that  $f^A$  is a time varying term and it vanishes after taking the time average of the volume force density [3]. According to our point of view, the mechanical momentum,  $P_{med}$  is carried by the electromagnetic field ( $P_{Minkowski} = P_{Abraham} + P_{med}$  when total momentum is transferred to an embedded particle from the background). For this reason,  $f^A$  is better expressed in time varying format and it should be.

The mechanical force is experienced by the embedded particle only when this  $P_{med}$  along with  $P_{Abraham}$  (field momentum) affects the interior dynamics of an embedded particle and the force distributes itself at the interior of the embedded particle via *self-Polarization and Magnetization* of the particle. That internal accurate mechanical force has been calculated in the main article using proposed modified Einstein-Laub stress tensor. In fact, Minkowski momentum density,  $G_M$  ( $= G_{Abraham} + f^A$ ) bears that mechanical momentum part ( $P_{med}$ ) in time varying form ( $f^A$ ). To remove this anomaly of total mechanical force from exterior, additional hidden quantities are

required with  $f_H$  [12], which can be avoided via the methods like Minkowski stress tensor or Ray tracing based force calculations.

#### **4. Pulling force in three dimensions**

A two dimensional (2D) model was used in the main text in order to illustrate the operation principles in a clear and easy manner. It demonstrates that all those results can be straightforwardly extended to three dimensional (3D) cases. In 3D cases, a small sphere is considered to be floating on the water-air interface, as shown in Fig. 2s, and the force exerted on it can be calculated by integrating Maxwell's stress tensor on an enclosed surface, or by using the ray tracing method. Here, only the results of the full wave method (FWM) are shown.

All the materials and geometric parameters are the same as in the 2D case used in the main text, i.e., medium-1 is air with  $n_1 = 1.0$ , medium-2 is water with  $n_2 = 1.33$ , and the scatterer sphere is made of polymer or silica with a moderate refractive index of  $n_3 = 1.45$ , with a radius  $r$ . The sphere is illuminated by a plane wave with a wavelength of  $\lambda_0 = 632.5$  nm. When the sphere has half volume in air and the other half immersed in water (if the scatterer center is above or below the air-water interface with a nonzero  $\Delta$ , the results are still available, as shown in main text), the force calculated by the Maxwell's stress tensor is shown in Fig. 2s. The results show that the force along the interface is negative in a wide range of incident angles.

Figure 2s (a) shows the field of the 3D sphere by three orthogonal slices along the  $x$ ,  $y$  and  $z$  directions, respectively. Here, we set the scatterer's center right on the water-air interface, i.e.  $\Delta = 0$ . The incident wave vector  $\mathbf{k}$  is in the  $xz$  plan, and the incident direction is  $\theta_1$  with respect to  $+x$  direction. Figure 2s (b) shows the change of  $F_x$  with incident angle  $\theta_1$  at different radius of  $r=0.4\mu\text{m}$  (red solid),  $1.0\mu\text{m}$  (blue dashed), and  $1.4\mu\text{m}$  (pink dash-dotted). One can see that negative scattering forces are present when  $r > 1.0 \mu\text{m}$  for both s- and p-polarizations. One also can find the trends of  $F_x \sim \theta_1$  which are familiar to those in 2D cases shown in Fig. 4 in the main text. When the scatterer is small enough, however, such as  $r = 0.4 \mu\text{m}$ ,  $F_x$  will be positive and very small, as shown by the red solid lines in Fig. 2s (b, c). This can also be understood easily from the "forward momentum amplification" method. With the decreasing of  $r$ , the cross section of the scatterer becomes smaller, so the amplitude of scattering force also becomes smaller. More importantly, smaller radius  $r$  means stronger diffraction when light projects on the scatterer, which reduces the part of momentum that can be amplified. In 2D case, there is also a critical value  $r_c$  to the radius  $r$  (which is about  $0.35\mu\text{m}$  for

the parameters adopted here). When  $r < r_c$ , no negative force can be achieved for any incident direction of  $\theta_1$ .

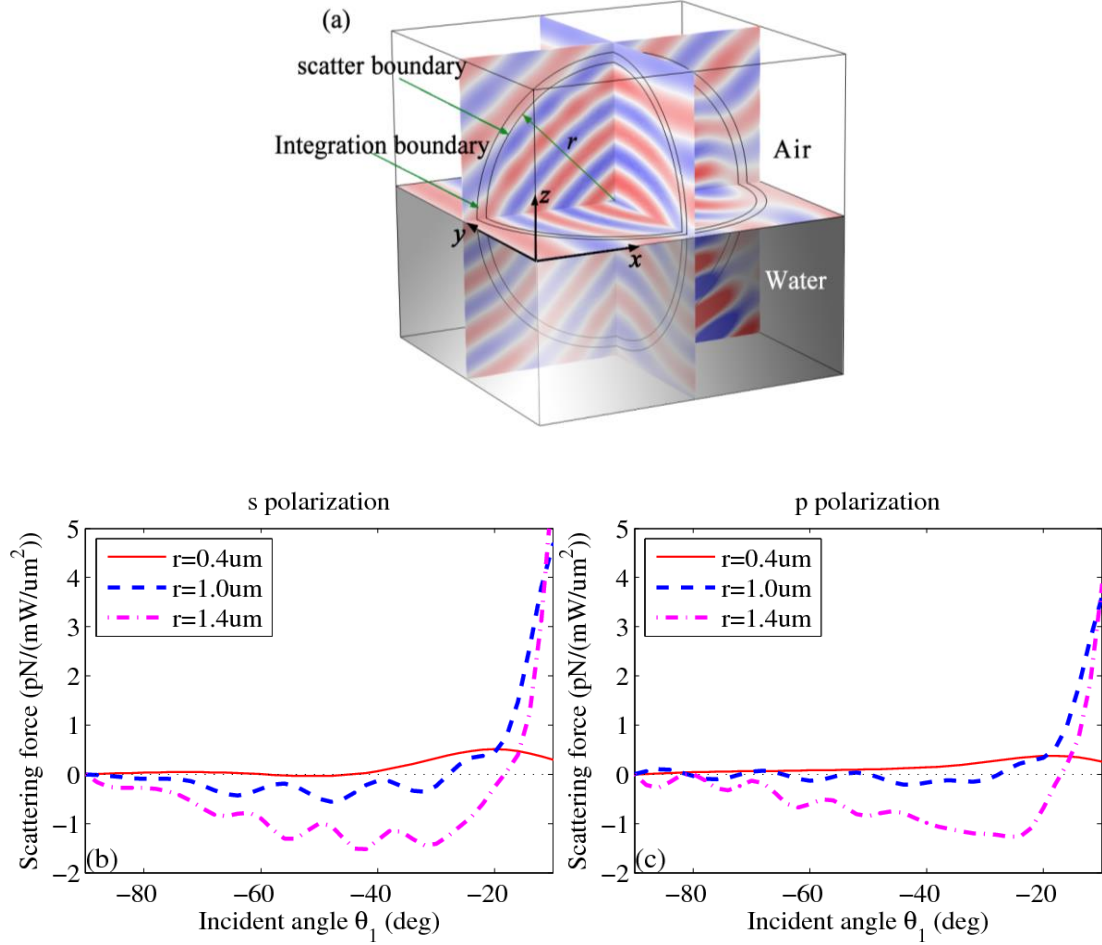


FIG. 2s (Color online). An optical scattering force in three dimensional structures. (a) Schematic illustration of the structure and fields by three orthogonal slices through the center of the scatter. The inner curves show the boundary of the scatter, and the outer curves show the integration boundary of Maxwell's stress tensor for force calculation.  $z = 0$  is the interface of water (below, darkened regions) and air (upper part). Blue and red colors on the slices show the field pattern of  $E_y$  for s-polarization with an incident direction of  $\theta_1 = -50$  degrees, and  $r = 1.4 \mu\text{m}$ . (b) An optical scattering force calculated by Maxwell's stress tensor for s-polarization on the enclosed surface for different sphere sizes of  $r = 0.4 \mu\text{m}$  (red line),  $1.0 \mu\text{m}$  (blue dashed) and  $1.4 \mu\text{m}$  (pink dash-dotted). (c) The same as (b) except for p-polarization.

In summary, the negative optical scattering force in 2D structures presented in the main text can be extended to 3D structures while still keeping all the appreciated features, such as vertical position  $\Delta$  in-sensitivity, and incident angle  $\theta_i$  in-sensitivity.

## **5. Stable manipulation on the interface by negative force**

In the main text, the optical scattering force  $F_x$  exerted on the scatterer is discussed, while the motion and stability of the scatterer on the interface are out of the scope of the main text, since the motion of a sphere on a liquid-gas interface may be a complex hydrodynamic process. Here we briefly show that it is possible to drive the scatterer with the optical scattering force stably on the water-air interface.

The motion of the scatterer on water-air interface can be divided along the normal and tangential directions. The results show that it is possible for the scatterer to float on the water-air interface stably, moving along the tangential direction simultaneously owing to the optical scattering force. Let us first analyze the stability of the scatterer in the normal direction.

In Ref. [13], it is shown that a sphere can be trapped in a surface energy well at water-air interface, and the stability of the sphere on the surface is determined by the depth of the well. For a sphere floating on the interface, the surface energy is contributed by three different parts[13].

The first part is the energy of sphere-air interface, which is

$$E_{s/a} = \sigma_{s/a} 2\pi r^2 (1 + \Delta / r).$$

The second part is the energy of the sphere/water interface, which is

$$E_{s/w} = \sigma_{s/w} 2\pi r^2 (1 - \Delta / r).$$

The third part is the negative energy of the missing water/air interface, which is

$$E_{w/a} = -\sigma_{w/a} \pi r^2 (1 - \Delta^2 / r^2)$$

where  $\sigma$  are the corresponding surface tensions between different materials, and  $r$  is the radius of the scatterer, and  $\Delta$  is the vertical position of the scatterer's center with respect to the water-air interface. Then one can calculate the total surface energy from the sum of three parts, which is (normalized by  $\sigma_{w/a} \pi r^2$ )

$$\tilde{E} = \frac{E_{s/a} + E_{s/w} + E_{w/a}}{\sigma_{w/a} \pi r^2} = \tilde{\Delta}^2 + 2(a-b)\tilde{\Delta} + 2a + 2b - 1,$$

with  $a = \sigma_{s/a} / \sigma_{w/a}$ , and  $b = \sigma_{s/w} / \sigma_{w/a}$ . The surface energy is normalized by  $E_{unit} = \sigma_{w/a} \pi r^2$ , and  $\tilde{\Delta} = \Delta / r$  is the vertical position normalized by the radius  $r$ . One can see that  $\tilde{E}$  is a parabolic curve and has a minimum value of

$$\tilde{E}_{min} = 2a + 2b - 1 - (a - b)^2 \quad \text{when} \quad \tilde{z} = b - a.$$

The energies are also obtained on the well edges of  $\tilde{E}(1) = 4a$  and  $\tilde{E}(-1) = 4b$ . At 25 degrees Celsius ( $\sigma_{w/a} = 72 \times 10^{-3} \text{ J/m}^2$ ,  $a \sim 0.49$ , and  $b \sim 0.14$ ), one can calculate  $\tilde{E}_{min} = 0.14$  at the position of  $\tilde{\Delta} = -0.35$ . Then one can calculate the depth of the energy well, which is (with the unit of  $E_{unit} = \sigma_{w/a} \pi r^2$ )

$$\Delta E_1 = E(1) - E_{min} = 1.96 - 0.14 = 1.82$$

$$\Delta E_{-1} = E(-1) - E_{min} = 0.56 - 0.14 = 0.42$$

When the radius of scatterer is  $r=2\mu\text{m}$ , the unit of surface energy is  $\sigma_{w/a} \pi r^2 = 9 \times 10^{-13} \text{ J}$ , which is much larger than the thermal energy  $k_B T \sim 4.1 \times 10^{-21} \text{ J}$  by a factor of  $2.2 \times 10^8$ . At the same time, the energy provided by the gravity is at the order of  $E_g = 4\pi / 3 r^3 \cdot \rho g r = 1.8 \times 10^{-18} \text{ J}$  for a scatterer with radius of  $2\mu\text{m}$ , and mass density of  $2.7 \times 10^3 \text{ kg/m}^3$ , which is also much smaller than the unit  $E_{unit}$  by a factor of  $5 \times 10^5$ . One can also find that the effect of the scattering force on the normal direction is also negligibly small. Therefore, it concludes that the surface energy well can trap the scatterer stably on the water-air interface.

Now, let us consider the tangential motion of the scatterer along the water-air interface. Apart from the optical scattering force, a resistance force will appear as soon as the scatterer begins to move on the interface. According to the well-known Stokes' formula, the drag force is[14]

$$F_d = B(\Delta) \cdot v,$$

where  $v$  is the velocity of the scatterer relative to water, and  $B(\Delta)$  is the friction coefficient, which is determined by the property of the liquid (water) and also the immersion depth of the scatterer in the liquid (water), i.e.[14],

$$B(\Delta) = 6\pi \cdot \mu \cdot r \cdot f(\Delta/r)$$

Here  $\mu$  is the dynamic viscosity of the fluid,  $r$  is the radius of the sphere, and  $f(\Delta/r)$  is a factor accounting for the hydrodynamic interaction of water and the sphere. The explicit form of  $f(\Delta/r)$  may not be easily obtainable, but its value can be given for several characteristic positions[14], such as  $f(0) = 0.5$ ,  $f(-1) = 0.716$ , and  $f(1) = 0$ .

For the case of  $\Delta = 0$ , one can write the motion equation of the scatterer driven by the optical scattering force and the drag force of water,

$$m \frac{dv}{dt} = F_{scat} - F_d = F_{scat} - 3\pi\mu r \cdot v,$$

with  $m$  being the mass of the scatter. Then, the final velocity of the scatterer can be calculated by setting  $dv/dt = 0$ ,

$$v_{final} = \frac{F_{scat}}{3\pi\mu r}$$

According to the results shown in Fig. 2s, one can suppose the optical scattering force is -1pN at the case of  $r=2\mu\text{m}$ . Supposing that the temperature is 300K, then the dynamic viscosity  $\mu$  of water is  $8 \times 10^{-4}$  Pa·s [15]. It is obtained that the final velocity is about 66 micrometer per second (or  $\mu\text{m/s}$ ), which can be observed and easily controlled in experiments. When the temperature is increased, the dynamic viscosity of water  $\mu$  decreases and a larger velocity is achieved.

It is expected that the scatterer can be suspended on the water-air interface stably, and driven by the optical scattering force. In the vertical direction, the surface energy well is deep enough to overcome the thermal Brownian motion and the gravitational energy. In the tangential direction, however, an observable velocity can be obtained by the total effect of the optical scattering force and the water drag force.

## 6. References

- [1] E. R. Tkaczyk, *Opt. Lett.* **37**, 972 (2012).
- [2] C. Baxter and R. Loudon, *J. Mod. Opt.* **57**, 830 (2010); R. N. C. Pfeifer, T. A. Nieminen, N. R. Heckenberg, and H. Rubinsztein-Dunlop, *Rev. Mod. Phys.* **79**, 1197 (2007).
- [3] P. W. Milonni and R. W. Boyd, *Advances in Optics and Photonics* **2**, 519 (2010).

- [4] R. Loudon, Phys. Rev. A **71**, 063802 (2005).
- [5] R. V. Jones and J. C. S. Richards, Proc. R. Soc. London Ser. A **221**, 480 (1954).
- [6] R. V. Jones and B. Leslie, Proc. R. Soc. London Ser. A **360**, 347 (1978).
- [7] B. A. Kemp, T. M. Grzegorzczuk, and J. A. Kong, Opt. Express **13**, 9280 (2005).
- [8] S. M. Barnett, Phys. Rev. Lett. **104**, 070401 (2010).
- [9] H. Minkowski, Nachr. Ges. Wiss. Goettingen, Math. Phys. Kl, , 53 (1908).
- [10] M. Abraham, Rend. Circ. Mat. Palermo **28**, 1 (1909); M. Abraham, Rend. Circ. Mat. Palermo **30**, 33 (1910).
- [11] R. Peierls, Proc. R. Soc. London Ser. A **355**, 141 (1977); R. Peierls, Proc. R. Soc. London Ser. A **347**, 475 (1976).
- [12] H. M. Lai, W. M. Suen, and K. Young, Phys. Rev. Lett. **47**, 177 (1981); M. Mansuripur, Proc. SPIE **8810**, 88100K, (San Diego, California, United States, 2013).
- [13] G. K. Batchelor, *Introduction to Fluid Dynamics* (Cambridge University Press, 1967).
- [14] B. Radoev, M. Nedjalkov, and V. Djakovich, Langmuir **8**, 2962 (1992).
- [15] J. Kestin, M. Sokolov, and W. A. Wakeham, J. Phys. Chem. Ref. Data **7**, 941 (1978); .